

RESEARCH ARTICLE

# $^1\text{H}$ NMR-based metabonomic profiling of rat serum and urine to characterize the subacute effects of carbamate insecticide propoxur

Yu-Jie Liang, Hui-Ping Wang, Ding-Xin Long, and Yi-Jun Wu

*Laboratory of Molecular Toxicology, State Key Laboratory of Integrated Management of Pest Insects and Rodents, Institute of Zoology, Chinese Academy of Sciences, Beijing, PR China*

## Abstract

Carbamate insecticide propoxur is widely used in agriculture and public health programs. To prevent adverse health effects arising from exposure to this insecticide, sensitive methods for detection of early stage organismal changes are necessary. We present here an integrative metabonomic approach to investigate toxic effects of pesticide in experimental animals. Results showed that propoxur even at low dose levels can induce oxidative stress, impair liver function, enhance ketogenesis and fatty acid  $\beta$ -oxidation, and increase glycolysis, which contribute to the hepatotoxicity. These findings highlight the applicability of  $^1\text{H}$  NMR spectroscopy and multivariate statistics in elucidating the toxic effects of propoxur.

**Keywords:** NMR, metabonomics, pesticide, subacute, toxicity

## Introduction

As a widely used carbamate pesticide, propoxur plays a vital role in agricultural programs and public health application. Due to its long-lasting and wide spectrum activity, propoxur is applied mainly in household pest control and for residual spraying in malaria eradication programs (Gupta et al. 2009). Although the benefits include enhanced agricultural productivity and reduction of insect-borne diseases, the overuse of propoxur can lead to adverse effect on non-target species, including severe acute and chronic poisoning of human and animal populations, which gives rise to concern for environmental pollution and health hazards of this insecticide (Thompson 1996).

Like other carbamates, propoxur reversibly blocks acetylcholinesterase activity (Shukla et al. 1998; Iyaniwura, 1991). In animal experiments, a single dose of  $1/10 \text{ LD}_{50}$  of propoxur caused 60% decrease in cholinesterase activity and marked disturbances in higher nervous functions (Thiesen et al. 1999) although the inhibited cholinesterase

activity usually returns to normal levels within a matter of hours (Padilla et al. 2007). In humans, the symptoms of propoxur poisoning include diarrhea, vomiting, abdominal pain, profuse sweating, salivation, blurred vision, and temporary paralysis of the extremities, which are typical for cholinergic overloading (El-Naggar et al. 2009). To prevent adverse health effects arising from repeated low-dose exposure to this insecticide, sensitive methods for detection of early stage organismal changes are necessary. In this study, a further investigation of the toxicity of the carbamates by metabonomics yields a new approach.

Metabonomics has been defined as “the quantitative measurement of the dynamic multiparametric metabolic response of living systems to pathophysiological stimuli or genetic modification” (Nicholson et al. 1999). It is a useful tool for assessing the effects of environmental stressors on the health of an organism (Viant et al. 2003), diagnosis of human diseases, and characterization of genetically modified animal models of disease (Tsang et al. 2006; Michael et al. 2005). Typically, nuclear

*Address for Correspondence:* Yi-Jun Wu, Institute of Zoology, Chinese Academy of Sciences, 1-5 Beichenxi Road, Beijing 100101, PR China.  
Tel: +86 10-64807251. Fax: +86 10 64807099. E-mail: wuyj@ioz.ac.cn

(Received 03 April 2012; revised 08 June 2012; accepted 16 June 2012)

magnetic resonance (NMR) spectroscopy is one of the analytical techniques widely used for metabonomic studies (Nicholson and Lindon 2008). With the automated data reduction and chemometric analysis such as principal components analysis (PCA) and partial least squares methods (Lindon et al. 2001; Lenz et al. 2007), the high-frequency  $^1\text{H}$  NMR spectra of biofluids can provide information on potentially hundreds of endogenous metabolites (Nicholls et al. 2001). Previous  $^1\text{H}$  NMR spectroscopy-based metabonomic analyses were applied successfully to analyze urine or serum of rats to characterize the dose-dependent effect of cadmium and mercury (Nicholson et al. 1983), nanoparticle copper (Lei et al. 2008), and light rare earth (Wu et al. 2005; Liao et al. 2007). The application of metabonomics is rapidly expanding to include the field of pesticide toxicity. It has been applied to investigate the metabolic response to the exposure of toxic organophosphorous compounds such as tri-phenyl phosphate and tri-butyl phosphate (Neerathilingam et al. 2010; Aliferis and Tokousbalides 2011; Alam et al. 2010). Our lab has used this tool to assess the toxic effects of pesticide mixture (Wang et al. 2009; Wang et al. 2011). In this current work, we applied a  $^1\text{H}$  NMR-based analytical strategy combined with multivariate pattern recognition (PR) techniques to develop a rapid-throughput *in vivo* screen of carbamate pesticide toxicity. Here, metabonomics technology was used to detect dose-dependent perturbations in the endogenous metabolite profiles of biofluids in propoxur-treated rats. This method for characterization of propoxur toxicity, will allow us to find mechanisms of toxicity of insecticide, as well as to identify potential biomarkers for early detection of toxic exposure.

## Materials and methods

### Reagents

Propoxur (2-isopropoxyphenyl *N*-methylcarbamate) (purity 97%) was a kind gift from the Institute of Chemical Industry (Hunan, China). 2, 2', 3, 3'-deuterio-trimethylsilylpropionic acid (TSP) and  $\text{D}_2\text{O}$  were purchased from Sigma Chemical Co. (St. Louis, MO, USA).

### Animals

Male Wistar rats weighing about  $200 \pm 10$  g used in the experiments were from Weitonglihua Animal Technology Company (Beijing, China). The animals were housed individually in plastic cages and kept under conventional conditions ( $22 \pm 3^\circ\text{C}$ ) temperature, 12 h light/12 h dark cycle,  $50 \pm 10\%$  relative humidity), with free access to standard food and drinking water. After 5-day acclimation, the rats were randomly allocated to four groups with 5 animals each group. For each treatment, three groups were randomly assigned to one of three levels of treatment (low, middle, and high dose) for propoxur treatment and one group assigned as the control. After the last treatment, the rats were transferred to individual metabolic cages and the urine samples were collected.

### Treatments

Based on data from previous studies showing that acute oral  $\text{LD}_{50}$  of propoxur was 85.1 mg/kg (Institoris et al. 2001), and referring to the earlier result that no-observed-adverse-effect level (NOAEL) value of propoxur is 10.00 mg/kg, which is equal to the value established by WHO/FAO Working Groups (1989), we chose the level of  $1/5 \text{ LD}_{50}$  as the highest dose in the present study to induce toxic signs in the treated rats. The other two dose levels were respectively chosen as  $1/5$  and  $1/25$  of the highest dose level; these two dose levels were expected to be lower than a NOAEL. Thus, the corresponding dose levels of propoxur for low-, middle-, and high- dose groups were respectively 0.68, 3.40, and 17.00 mg/kg body weight per day.

Propoxur was dissolved in corn oil and applied per os by gavage in a volume of 1 ml/kg body weight. The control group received an equivalent volume of corn oil (vehicle control). All animals were treated consecutively for 28 days.

All animal procedures were implemented in accordance with current China legislation and approved by the Institute of Zoology Animals Medical Ethics Committee.

### Sample collection

After last dosing, 24-h (9 a.m. to 9 a.m. next day) urine samples of each rat were collected into ice-cold vessel containing 1% sodium azide (0.1 ml) to prevent bacterial contamination. The urine collected was then centrifuged at  $3000g$  for 10 min to remove any particulate matter, after which aliquots were taken from each sample and stored at  $-80^\circ\text{C}$  prior to NMR analysis.

Twenty four hours after the final administration, all rats were terminated by exsanguination under isoflurane anesthesia. During the process, blood samples were collected. Serum samples were isolated by centrifuging at  $2000g$  for 15 min at  $4^\circ\text{C}$ . Aliquots of the samples were frozen at  $-80^\circ\text{C}$  for the following NMR spectroscopy and clinical chemistry analysis.

Liver and kidney tissues were immediately dissected and fixed in 10% (v/v) buffered neutral formalin solution for histopathological examination.

### Clinical chemistry and histological analysis

Biochemical parameters of serum samples were analyzed on an Autolab-PM4000 Automatic Analyzer (AMS Co., Rome, Italy).

Fixed tissues were processed into paraffin wax, then cut into sections of 5–6  $\mu\text{m}$  thickness and stained with hematoxylin-eosin. Light microscopic examination of the sections was then carried out.

### $^1\text{H}$ NMR spectroscopic measurement of urine sample

Four hundred microliters (400  $\mu\text{l}$ ) of each urine sample were mixed with 200  $\mu\text{l}$  phosphate buffer solution (PBS) ( $0.2\text{M Na}_2\text{HPO}_4/0.2\text{M NaH}_2\text{PO}_4$ , pH 7.4) to minimize variations in sample pH. The urine-buffer mixture was allowed to stand for 10 min and then centrifuged at  $3500g$  for 5 min at  $4^\circ\text{C}$  in order to remove any precipitates.

Aliquots of the supernatants (500  $\mu$ l) from each urine sample were mixed with 50  $\mu$ l of TSP dissolved in D<sub>2</sub>O solution (1 mM, final concentration). The TSP acted as the internal chemical shift reference ( $\delta_{\text{H}}$  0.0), whereas D<sub>2</sub>O was used for deuterium lock signal for NMR spectrometer. All <sup>1</sup>H NMR spectra data were recorded on a Bruker-Av600 spectrometer (Bruker Co., Germany) at 298 K. Water signals were suppressed by presaturation (Wei et al. 2008).

### <sup>1</sup>H NMR spectroscopic measurement of serum samples

Four hundred microliters (400  $\mu$ l) of serum samples were placed in 5-mm NMR tubes and combined with 50  $\mu$ l D<sub>2</sub>O for locking signal and 50  $\mu$ l PBS to minimize variations in sample pH. All NMR spectra were acquired on spectrometer operating at 600.13 MHz. Water signals and broad protein resonances were suppressed by a combination of presaturation and the Carr-Purcell-Meiboom-Gill (CPMG) spin-echo pulse sequence (RD-90°( $\tau$ -180°- $\tau$ )<sub>n</sub> acquisition) (Nicholson et al. 1995).

### Data reduction of <sup>1</sup>H NMR spectra

All <sup>1</sup>H-NMR spectra were manually phased, baseline corrected, and then each spectral region between 10–0.2 parts per million (ppm) was segmented into each width of 0.04 ppm (urine) or 0.005 ppm (serum) using MestReC (version 2.3, Mestrelab Research, A Coruna, Spain). Typically, 32 free induction decays (FIDs) were collected into 64 k data points with a relaxation delay of 5 s and an acquisition time of 0.91 s. Prior to Fourier transformation, the FIDs were multiplied by an exponential function with a 0.3 Hz line-broadening factor, and all spectra were then referenced to the CH<sub>3</sub> resonance of creatine at  $\delta$ 3.05 (Wei et al. 2009). For urine spectra analysis, we scaled the normalized metabolite concentrations according to the approximate population average concentration of creatinine, to remove the effects of variation in the suppression of water resonance and the effects of variation in

the urea signal, and the region between 4.2 to 6.0 ppm was removed prior to PR analysis. The remaining 198 spectral segments were scaled to the total integrated area of each spectrum. For serum samples, the region of the spectrum that included the water signal ( $\delta$ 4.4–5.2) was also removed from the analysis. The remaining spectral segments were scaled to total integrated area of each spectrum.

### PR of the <sup>1</sup>H-NMR spectra

PCA with mean centering was processed with the software SIMCA-P version 11.5 (Umetrics AB, Umea, Sweden). In the PCA model, data were visualized by using the PC scores and loading plots (Beckonert et al. 2003). Two-dimensional PC score plots facilitated visualization of dose-related patterns or clusters of samples, while corresponding PC loadings represented single NMR spectral regions that characterized underlying metabolic changes by showing the influence of the different spectral areas on the PCs. Thus, a score plot of PC1 vs. PC2 provides the most efficient two-dimensional score plot representation of the information contained in the data set (Waters et al. 2005; Waters et al. 2002). The corresponding loading plots could identify metabolites which are considered to have a significant contribution to the position of the samples in the score plot and hence more attention should be paid to these variables (Coen et al. 2003).

## Results

### Body weight and clinical chemistry

There were no obvious clinical signs with any of the animals throughout the dosing period, and all animals survived until sacrifice. Body weights of treatment groups did not differ from the control values in either low or middle dose groups during the experiment, although a slight decrease was observed in the high dose group of rats after 3 weeks dosing (data not shown). The result

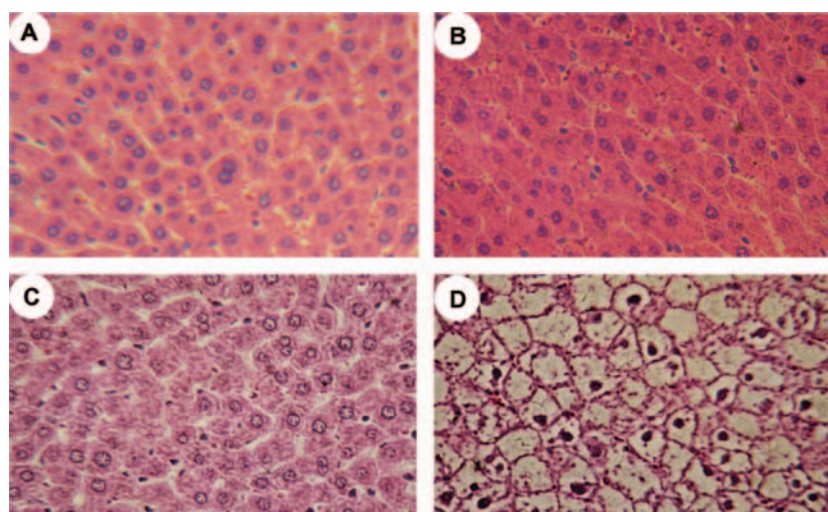


Figure 1. Photomicrograph of liver tissue sections of rats. (A) Control rats demonstrate normal structure of hepatocytes; (B) Rats treated with low-dose of propoxur (0.68 mg/kg) exhibited nearly normal structure of hepatocytes; (C) Rats treated with mid-dose of propoxur (3.4 mg/kg) exhibited faintly stained cytoplasmic nuclei; (D) Rats treated with high-dose propoxur (17 mg/kg) exhibited vacuolated cytoplasm nuclei and karyopyknosis of hepatocytes. (Magnification, 200  $\times$ ).



of blood chemical analysis showed that cholinesterase activity was significantly inhibited by propoxur at the tested dose levels although other parameters such as serum glutamic-oxaloacetic transaminase, glutamic pyruvic transaminase, alkaline phosphatase, and blood urea nitrogen, were not affected in any group (data not shown).

### Histopathology

Liver tissue sections of rats treated with different doses of propoxur for 28 consecutive days are shown in Figure 1. Microscopy examination found that liver parenchymal cells from the rats of the high dose group changed with hepatocellular necrosis and vacuolation (Figure 1D). Some animals were noted to show slightly histopathological changes caused by the pesticide, which was identified in rats of the middle dose group (Figure 1C). No discernible differences were found in

the livers between low dose exposed and non-exposed control rats (Figure 1A and 1B). None of the propoxur treatment groups demonstrated pathological changes associated with kidney damage (data not shown).

### <sup>1</sup>H NMR spectra and PR analysis of urine samples show dose-related biochemical alteration of propoxur-treated rats

After 28-day treatment, the dose-related toxicity of propoxur was investigated by applying PCA to the datasets containing NMR spectra of urine from control and all of the pesticide-treated animals (Figure 2). The valuable information on endogenous biochemical changes of samples based on the similarities of biochemical profiles was visualized by PCA to map the NMR spectra into a low dimensional metabolic space.

PCA scores plot of the NMR spectra of urine samples showed a distinct clustering of the various groups

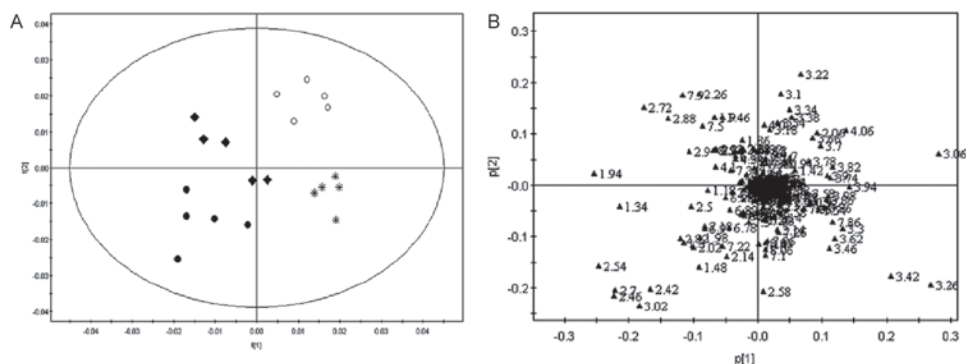


Figure 2. PCA scores plot (A) and corresponding loadings plot (B) based on the <sup>1</sup>H NMR spectra of rat urine. The rats were treated with propoxur at doses of 0 mg/kg (○), 0.68 mg/kg (\*), 3.4 mg/kg (◆), and 17 mg/kg (●) respectively for consecutive 28 days. The numbers refer to peak chemical shifts of the discriminating features include: 1.34 ppm, 1.94 ppm, 1.46 ppm, 2.54, 2.70 ppm, 2.42, 3.02 ppm, 2.46 ppm, 2.9 ppm, 8.5 ppm, 4.06, 3.06 ppm, 3.24, 3.40 ppm, 3.26, 3.42 ppm, 3.58 ppm, 2.88 ppm.

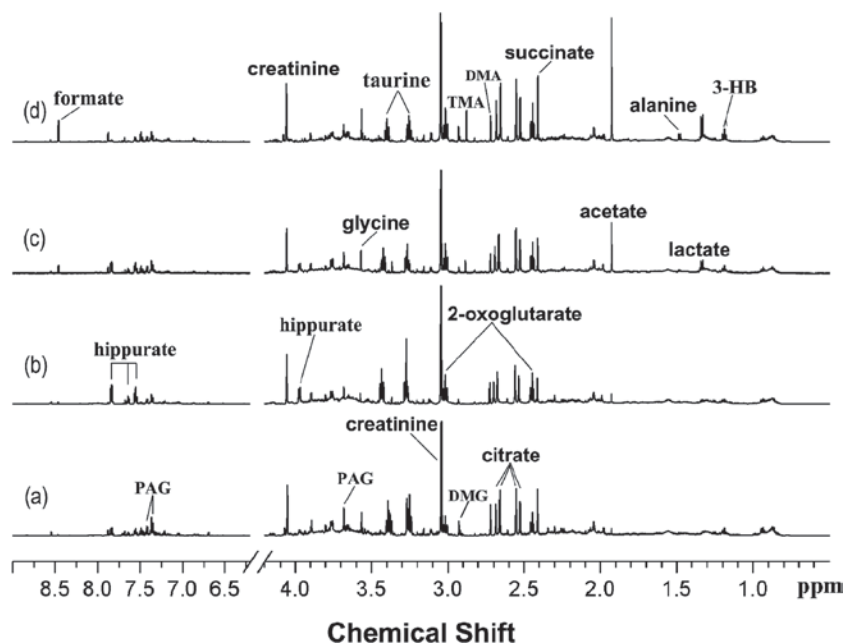


Figure 3. Typical 600 MHz <sup>1</sup>H NMR spectra of rat urine. The rats were treated with propoxur at doses of 0 mg/kg (a), 0.68 mg/kg (b), 3.4 mg/kg (c), and 17 mg/kg (d) respectively. Abbreviations: TMA, trimethylamine; DMA, dimethylamine; DMG, dimethylglycine.

(Figure 2A). Both mid- and high-dose group readily separated from the control group along PC1 and PC2 axis. Even the low-dose group exhibited separation of some urine profiles from the cluster of control spectra. The loading plots of the PCA results from urine samples showed those spectral regions that contribute most to separation of samples in scores plot (Figure 2B). The dominant increase in the intensity of lactate (1.34 ppm)

with concomitant elevation in the signal of the acetate (1.94 ppm) and alanine (1.46 ppm) were responsible for the separation of the mid- and high-dose group from control. Also, increased concentrations of citrate (2.54, 2.70 ppm), 2-oxoglutarate (2-OG) (2.42, 3.02 ppm), succinate (2.46 ppm), dimethylglycine (DMG) (2.9 ppm) and formate (8.46 ppm) were identified in the mid- and high- dose group. Additionally, reduction

Table 1. Summary of the propoxur-induced variations in the endogenous urinary metabolites.

Major metabolites	Chemical shifts (ppm)	Dose levels (mg/kg/day)		
		0.68	3.40	17.00
Lactate	1.34 (d)	–	↑	↑*
Alanine	1.46 (d)	–	↑	↑
Acetate	1.94 (s)	–	↑*	↑*
Succinate	2.42 (s)	–	–	↑*
Citrate	2.54, 2.70 (d)	–	↑	↑*
2-oxoglutarate	2.46, 3.02 (t)	–	↑*	↑*
Taurine	3.26, 3.42 (t)	↑	–	–
Glucose	3.22, 3.34, 3.54, 3.74 (m)	–	↓*	↓*
Fructose	3.62, 3.66, 3.70, 3.78, 3.82, 3.90 (m)	–	↓	↓
N-acetylglutamate	1.90, 1.98, 2.02, 2.38 (m)	–	↑	↑
Aspartate	2.82 (s)	–	↑	↑
Asparagine	2.86, 2.94 (d)	–	↑	↑
Trimethylamine	2.88 (s)	–	↑	↑
Proline	3.30 (s)	–	↑	↑
Glycine	3.46 (s)	–	↑	–
Hippurate	3.98, 7.66, 7.86 (m)	↑*	↑	–
Phenylacetylglycine	3.68, 7.35, 7.42 (m)	–	↓	↓
Formate	8.48 (s)	–	↑	↑

Changes are relative to control samples: –, no change; ↓, decrease; ↑, increase. The integral values for each segmented region of chemical shift were represented for each metabolite resonance. Comparisons among groups were performed by ANOVA with post hoc analysis using Dunnett's test. \* $p < 0.05$  was considered significant, compared with control.

Abbreviations: s: singlet; d: doublet; t: triplet; m: multiplet.

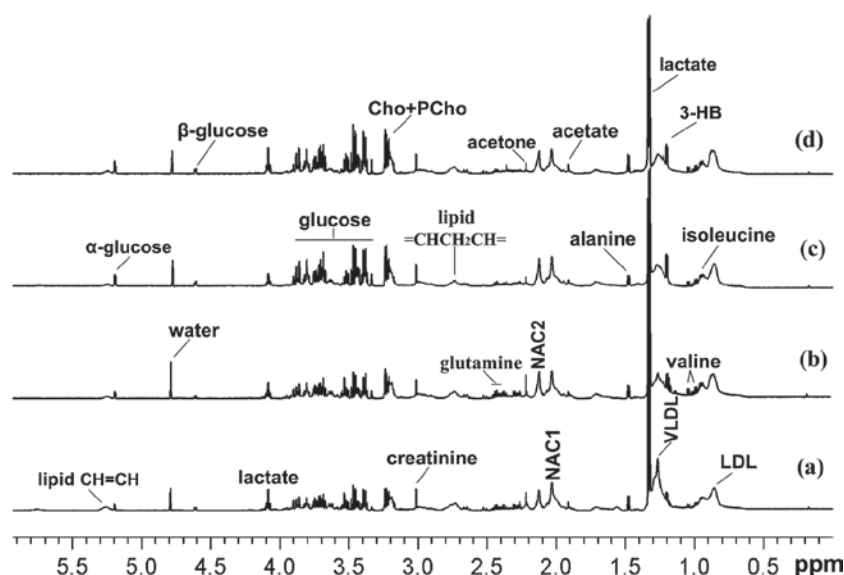


Figure 4. Series of serum CPMG  $^1\text{H}$  NMR spectra ( $\delta$  0–6) from rats. The rats were treated with propoxur at doses of 0 mg/kg (a), 0.68 mg/kg (b), 3.4 mg/kg (c), and 17 mg/kg (d). Signal variations are shown in the resonances of lactate, alanine, acetate, acetoacetate, glutamine. Key: 3HB, 3-D-hydroxybutyrate; LDL, low-density lipoprotein; VLDL, very low-density lipoprotein; NAC1 and NAC2, composite N-acetyl signals from glycoproteins; Cho, choline; PCho, phosphocholine.

in the concentration of glucose also contributed to this separation from control. Elevation of  $\beta$ -glucose (3.24, 3.40 ppm), taurine (3.26, 3.42 ppm), and hippurate (3.98, 7.66, and 7.86 ppm) contributed to separation of the low-dose groups. The series of visual urine spectra demonstrated a slight increase of 3-D-hydroxybutyrate (3HB) (1.20 ppm), glycine (3.58 ppm) and trimethylamine (2.88 ppm) (Figure 3). The propoxur induced perturbations in the biochemical composition of urine, the results of which are summarized in Table 1, demonstrating higher urinary concentrations of lactate, acetate, citrate and lowest level of glucose exhibited in a dose-dependent fashion.

### $^1\text{H}$ NMR spectra and PR analysis of serum samples from propoxur-treated rats

Utilization of the CPMG pulse in the acquisition of serum spectra reduced the effect of large macromolecules that typically display reduced mobility on the NMR time scale. As a result, a typical  $^1\text{H}$  CPMG NMR spectrum in Figure 4 shows several low molecular weight metabolites from the serum sample. Most resonances have been previously assigned including the major low molecular weight metabolites that dominated the spectra composed of lactate, choline/phosphocholine, pyruvate, citrate, acetate, creatine, formate, fatty acids, and some amino acids. However, visual inspection of these spectra

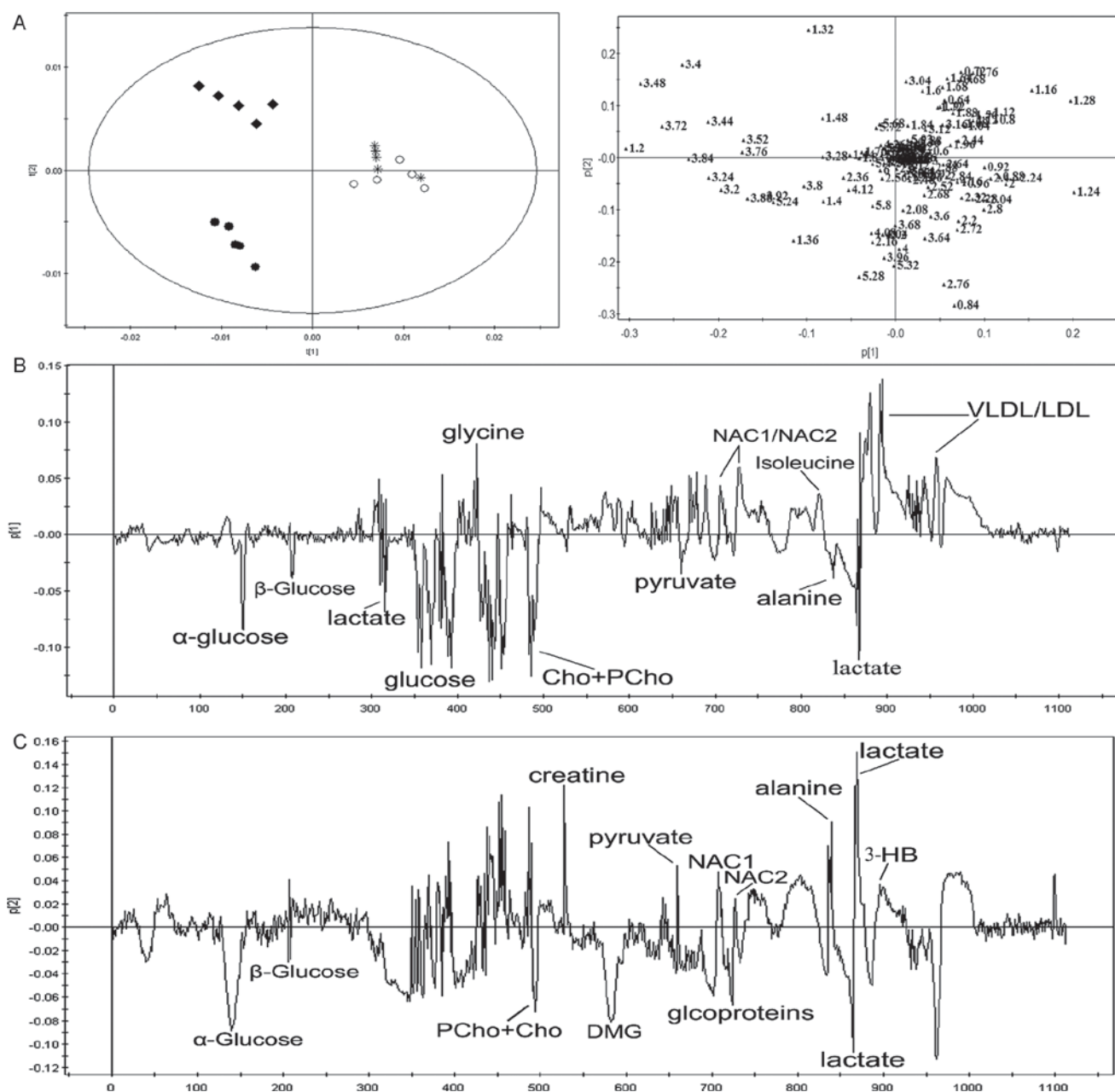


Figure 5. Scores plot (A, left) and corresponding loadings scatter plot (A, right) based on serum CPMG  $^1\text{H}$  NMR spectra obtained from treated rats. The rats were treated with propoxur at doses of 0 mg/kg ( $\circ$ ), 0.68 mg/kg ( $*$ ), 3.4 mg/kg ( $\blacklozenge$ ), and 17 mg/kg ( $\bullet$ ) respectively for consecutive 28 days. Loadings line plots (B and C) from PCA model corresponding to the PC1 and PC2 respectively, showing the prominent changes contributing to the discrimination.

did not present any clear differences among the dose levels used in this study.

Figure 5 shows the PC scores and loading plots obtained from analysis of the serum samples. A plot of PCA scores derived from the  $^1\text{H}$  NMR spectra showed that three dose groups clustered very tightly together, and the control group forms a tight cluster while the cluster of low dose group is more close to the control group (Figure 5A). PC1 captured the greatest variation in the spectra of control and propoxur-treated animals while PC2 was the most influential in distinguishing those animals of mid- and high- dose groups. This suggested that both mid- and high- dose groups exhibited altered biochemical composition after rats were exposed to propoxur for 28 consecutive days.

Using the PCA weights, line plots were generated to identify the resonances from these metabolites that are most influential in discrimination of these responses. The line plots respectively represented the first and the second component (Figure 5B and 5C). Here, the variables with a large negative value are likely to be correlated with the mid- and high- dose groups, while those with positive values are probably corresponded to the control or low-dose group (Figure 5B). The prominent changes in endogenous serum metabolites were identified from the loading line plots. These plots correspond to the first component that displayed increased levels of lactate (1.34 and 4.11 ppm), pyruvate (2.38 ppm), betain (3.27 and 3.90 ppm), choline (3.20 ppm), phospholine (3.22 ppm), and glucose (3.10–4.50 ppm), the decreased levels of amino acids (valine, leucine/isoleucine, glutamine, and glycine), and the composite N-acetyl signals from glycoproteins and lipid, which contributed to the separation of mid- and high-dose groups from control group (Figure 5B). Additionally, the separation of the mid-dose group from high-dose group along PC2 was demonstrated (Figure 5C). The variables with a large negative value are positively correlated with the high-dose group, while those with positive values are positively correlated with the mid-dose group. The highest levels of lactate, choline/phosphocholine,  $\alpha$ - and  $\beta$ -glucose were observed in rats treated with high-dose propoxur whereas the strongest signal of creatine, alanine, and pyruvate were seen in the mid-dose treated animals (Figure 5C).

## Discussion

Hepatotoxicity induced by pesticides especially carbamates/organophosphates are of great concern. The data in this present study suggests that propoxur at high dose can induce hepatotoxicity, which was confirmed by the result of histopathological examination. The highest dose of the pesticide used in this study is 17 mg/kg, which is slightly higher than the NOAEL value, while the other doses used are far lower than the NOAEL, which are insufficient to induce observable histopathological change. However, the following metabonomic profile analysis from the urine and serum samples not only

validated the above histopathological findings, but also further revealed the toxicity of propoxur exposure even at lower dose levels.

The PR technique used here successfully and clearly separated high-dose, mid-dose, and low-dose group from the control and each other in the  $^1\text{H}$  NMR spectra of urine samples, which indicates alteration of biochemical composition or different toxicological modes-of-action in the rats after 28-day accumulative exposure to propoxur. Through the loading plots or spectra, we found the apparent biochemical changes include elevation of the single intensity of lactate, acetate, and other urine metabolites.

The increased tricarboxylic acid (TCA) cycle intermediates, such as citrate, succinate, and 2-OG, may indicate that the activity of TCA cycle enzymes in hepatocytes were influenced by propoxur, which may have affected energy metabolism in liver. Acetate is an end product of fatty acid oxidation. It is also produced from glycerol-phospholipid and pyruvate metabolism (Bradford et al. 2008). The increase of urinary acetate levels suggests that the metabolic pathway to acetyl-CoA was inhibited and energy status of liver was disturbed. It is postulated that the energy metabolism was shifted toward ketone body formation, which can be used as an alternative energy source. The abnormal elevation of the 3HB validated this switch because 3HB is one of the ketones produced primarily by liver oxidation of fatty acids. Usually, 3HB is a hallmark of enhanced  $\beta$ -oxidation and a clue to liver malfunction. Hence, the high dose propoxur may disturb carbohydrate metabolism, causing glucose to be ineffectively utilized and eventually leads to the increase of ketone body formation.

However, serum sample PCA scores plot showed that low-dose groups overlapped with control, suggesting the same kind of metabolic profiles between these two groups. These findings are consistent with that the low-dose group did not produce significant histopathological changes. Although the mid-dose was far below the NOAEL, we detected some significant metabonomic changes related to hepatotoxicity.

As a result of CPMG sequence suppression, the broad peak regions of very low-density lipoprotein (VLDL) and low-density lipoprotein (LDL) were considerably restrained. However, the signal intensities of VLDL/LDL of vehical control group were much stronger than those of the mid- and high-dose propoxur groups. The drop in serum LDL/VLDL in the high-dose group suggested that carbohydrate metabolism was altered. It is possible that propoxur directly affected the key enzymes of carbohydrate metabolism (Solanky et al. 2003). It was reported that propoxur induced the generation of free radicals and alterations in antioxidants or oxygen free radical, which lead to lipid peroxidation enhancement and malondialdehyde (MDA) levels increase (Siroki et al. 2001) and induced haematological changes, indicating the damage of liver in rats (Institóris et al. 2002). We deduced that this modification may contribute to the hepatotoxicity observed in the rats of the high-dose group. Accumulation of propoxur probably caused oxidative damage in liver tissues under



continuous administration, which was in concordance with the histological findings.

All the results above showed that  $^1\text{H}$  NMR spectra of serum samples can provide detailed toxicological information on rats exposed to propoxur. The metabonomic data obtained from the present study provides new important mechanistic clues to the effects of propoxur on liver metabolism and energy utilization which may be important for understanding the pathogenesis of liver injury. This evidence demonstrates that subacute administrations of mid- and high-dose propoxur might disturb antioxidative defense systems and increase lipid peroxidation in liver tissues of rats. A recent study reported that propoxur could injure CHO-K1 cells via oxidative stress by the significant increase in MDA production (Maran et al. 2010), suggesting that propoxur induced the lipoperoxidation *in vitro* and induction of oxidative stress might be related to their cytotoxic effects (Gahelnabi et al. 2000). Previous *in vivo* studies (Maran et al. 2009; Seth et al. 2001) showed that propoxur insecticide caused oxidative stress through the generation of free radicals and changes in antioxidant enzymes and oxygen-free radical scavengers. One clinical investigation consisted of 30 patients of propoxur poisoning observed the increased blood lipid peroxidation products (for example, MDA), which indicates the oxidative stress after human poisoning with propoxur (Seth et al. 2000). On the other hand, these findings indicated that the elevated serum lactate, pyruvate, choline, and phosphocholine as well as the decreased alanine and glucose could serve as the possible biomarkers for liver damage caused by propoxur.

Comparison of NMR-PR data with histopathological changes in rats suggests that significant changes of histopathology could only be observed in the rats of the high-dose group, but the current NMR-PR is able to detect a difference at the mid-dose group and predict hepatotoxicity. Overall, urine samples facilitate no-invasion monitoring of metabonomic modification and should be chosen first, whereas serum sample changes represent more chronic or long-term snapshots of the system (Solanky et al. 2003). The advantages of metabonomics approach including sensitivity, speed, and high-throughput nature could favor it for detection of clinically relevant biomarkers and rapid *in vivo* screening. Therefore the application of metabonomics in the study of pesticide toxicity has apparent benefits over traditional classical toxicology.

## Acknowledgements

The authors would like to thank Huang Huang and Dr. Jill Wentzell for kindly polishing the English of the manuscript.

## Declaration of interest

This work was partly supported by the CAS Innovation Program (No. KZCX2-EW-404), the SKLECE program (No. KF2010-16), and NSFC program (No. 31071919).

## References

- Alam TM, Kathleen Alam M, Neerathilingam M, Volk DE, Sarkar S, Shakeel Ansari GA, Luxon BA. (2010).  $^1\text{H}$  NMR metabonomic study of rat response to tri-phenyl phosphate and tri-butyl phosphate exposure. *Metabolomics* 6:386–394.
- Aliferis KA, Tokousbalides M. (2011). Metabolomics in pesticide research and development: review and future perspectives. *Metabolomics* 7:35–53.
- Beckonert OE, Bollard M, Ebbels TMD, Keun HC, Antti H, Holmes E, Lindon JC, Nicholson JK. (2003). NMR-based metabonomic toxicity classification: hierarchical cluster analysis and k-nearest-neighbour approaches. *Anal Chim Acta* 490:3–15.
- Bradford BU, O'Connell TM, Han J, Kosyk O, Shymonyak S, Ross PK, Winnike J, Kono H, Rusyn I. (2008). Metabolomic profiling of a modified alcohol liquid diet model for liver injury in the mouse uncovers new markers of disease. *Toxicol Appl Pharmacol* 232:236–243.
- Coen M, Lenz EM, Nicholson JK, Wilson ID, Pognan F, Lindon JC. (2003). An integrated metabonomic investigation of acetaminophen toxicity in the mouse using NMR spectroscopy. *Chem Res Toxicol* 16:295–303.
- El-Naggar Ael-R, Abdalla MS, El-Sebaey AS, Badawy SM. (2009). Clinical findings and cholinesterase levels in children of organophosphates and carbamates poisoning. *Eur J Pediatr* 168:951–956.
- Gahelnabi M, Mousa H, Ali B. (2000). Comparative toxicity of the carbamate insecticides bendiocarb and propoxur in Nubian goats. *Pakistan J Biol Sci* 3:2193–2196.
- Gupta S, Garg GR, Bharal N, Mediratta PK, Banerjee BD, Sharma KK. (2009). Reversal of propoxur-induced impairment of step-down passive avoidance, transfer latency and oxidative stress by piracetam and ascorbic acid in rats. *Environ Toxicol Pharmacol* 28:403–408.
- Institóris L, Papp A, Siroki O, Banerjee BD, Dési I. (2002). Immuno- and neurotoxicological investigation of combined subacute exposure with the carbamate pesticide propoxur and cadmium in rats. *Toxicology* 178:161–173.
- Institóris L, Siroki O, Undeger U, Basaran N, Banerjee BD, Dési I. (2001). Detection of the effects of repeated dose combined propoxur and heavy metal exposure by measurement of certain toxicological, haematological and immune function parameters in rats. *Toxicology* 163:185–193.
- Iyaniwura TT. (1991). Relative inhibition of rat plasma and erythrocyte cholinesterases by pesticide combinations. *Vet Hum Toxicol* 33:166–168.
- Lei R, Wu C, Yang B, Ma H, Shi C, Wang Q, Wang Q, Yuan Y, Liao M. (2008). Integrated metabolomic analysis of the nano-sized copper particle-induced hepatotoxicity and nephrotoxicity in rats: a rapid *in vivo* screening method for nanotoxicity. *Toxicol Appl Pharmacol* 232:292–301.
- Lenz EM, Wilson ID. (2007). Analytical strategies in metabonomics. *J Proteome Res* 6:443–458.
- Liao P, Wei L, Zhang X, Li X, Wu H, Wu Y, Ni J, Pei F. (2007). Metabolic profiling of serum from gadolinium chloride-treated rats by  $^1\text{H}$  NMR spectroscopy. *Anal Biochem* 364:112–121.
- Lindon JC, Holmes E, Nicholson JK. (2001). Pattern recognition methods and applications in biomedical magnetic resonance. *Prog Nucl Magn Reson Spectrosc* 39:1–40.
- Maran E, Fernández M, Barbieri P, Font G, Ruiz MJ. (2009). Effects of four carbamate compounds on antioxidant parameters. *Ecotoxicol Environ Saf* 72:922–930.
- Maran E, Fernández-Franzón M, Font G, Ruiz MJ. (2010). Effects of aldicarb and propoxur on cytotoxicity and lipid peroxidation in CHO-K1 cells. *Food Chem Toxicol* 48:1592–1596.
- Michael RP, Jonathan DC, Hannah MM, Russell JM, David AP, Julian LG. (2005). High Resolution  $^1\text{H}$  NMR-based Metabolomics Indicates a Neurotransmitter Cycling Deficit in Cerebral Tissue from a Mouse Model of Batten Disease. *J Biol Chem* 280:42508–42514.
- Neerathilingam M, Volk DE, Sarkar S, Alam TM, Alam MK, Ansari GA, Luxon BA. (2010).  $^1\text{H}$  NMR-based metabonomic investigation of tributyl phosphate exposure in rats. *Toxicol Lett* 199:10–16.



- Nicholls AW, Holmes E, Lindon JC, Shockcor JP, Farrant RD, Haselden JN, Damment SJ, Waterfield CJ, Nicholson JK. (2001). Metabonomic investigations into hydrazine toxicity in the rat. *Chem Res Toxicol* 14:975–987.
- Nicholson JK, Foxall PJ, Spraul M, Farrant RD, Lindon JC. (1995). 750 MHz <sup>1</sup>H and <sup>1</sup>H-<sup>13</sup>C NMR spectroscopy of human blood plasma. *Anal Chem* 67:793–811.
- Nicholson JK, Kendall MD, Osborn D. (1983). Cadmium and mercury nephrotoxicity. *Nature* 304:633–635.
- Nicholson JK, Lindon JC, Holmes E. (1999). 'Metabonomics': understanding the metabolic responses of living systems to pathophysiological stimuli via multivariate statistical analysis of biological NMR spectroscopic data. *Xenobiotica* 29:1181–1189.
- Padilla S, Marshall RS, Hunter DL, Lowit A. (2007). Time course of cholinesterase inhibition in adult rats treated acutely with carbaryl, carbofuran, formetanate, methomyl, methiocarb, oxamyl or propoxur. *Toxicol Appl Pharmacol* 219:202–209.
- Nicholson JK, Lindon JC. (2008). Systems biology: metabonomics. *Nature* 455:1054–1056.
- Seth V, Banerjee BD, Bhattacharya A, Chakravorty AK. (2000). Lipid peroxidation, antioxidant enzymes, and glutathione redox system in blood of human poisoning with propoxur. *Clin Biochem* 33:683–685.
- Seth V, Banerjee BD, Chakravorty AK. (2001). Lipid peroxidation, free radical scavenging enzymes, and glutathione redox system in blood of rats exposed to propoxur. *Pestic Biochem Physiol* 71:133–139.
- Shukla Y, Baqar SM, Mehrotra NK. (1998). Carcinogenicity and co-carcinogenicity studies on propoxur in mouse skin. *Food Chem Toxicol* 36:1125–1130.
- Siroki O, Undeger U, Institóris L, Nehéz M, Basaran N, Nagymajtényi L, Dési I. (2001). A study on geno- and immunotoxicological effects of subacute propoxur and pirimicarb exposure in rats. *Ecotoxicol Environ Saf* 50:76–81.
- Solanky KS, Bailey NJ, Beckwith-Hall BM, Davis A, Bingham S, Holmes E, Nicholson JK, Cassidy A. (2003). Application of biofluid <sup>1</sup>H nuclear magnetic resonance-based metabonomic techniques for the analysis of the biochemical effects of dietary isoflavones on human plasma profile. *Anal Biochem* 323:197–204.
- Thiesen FV, Barros HM, Tannhauser M, Tannhauser SL. (1999). Behavioral changes and cholinesterase activity of rats acutely treated with propoxur. *Jpn J Pharmacol* 79:25–31.
- Thompson HM. (1996). Interactions between pesticides; a review of reported effects and their implications for wildlife risk assessment. *Ecotoxicology* 5:59–81.
- Tsang TM, Woodman B, McLoughlin GA, Griffin JL, Tabrizi SJ, Bates GP, Holmes E. (2006). Metabolic characterization of the R6/2 transgenic mouse model of Huntington's disease by high-resolution MAS <sup>1</sup>H NMR spectroscopy. *J Proteome Res* 5:483–492.
- Viant MR, Rosenblum ES, Tieerdema RS. (2003). NMR-based metabolomics: a powerful approach for characterizing the effects of environmental stressors on organism health. *Environ Sci Technol* 37:4982–4989.
- Wang HP, Liang YJ, Long DX, Chen JX, Hou WY, Wu YJ. (2009). Metabolic profiles of serum from rats after subchronic exposure to chlorpyrifos and carbaryl. *Chem Res Toxicol* 22:1026–1033.
- Wang HP, Liang YJ, Zhang Q, Long DX, Li W, Li L, Yang L, Yan XZ, Wu YJ. (2011). Changes in metabolic profiles of urine from rats following chronic exposure to anticholinesterase pesticides. *Pestic Biochem Physiol* 101:232–239.
- Waters NJ, Holmes E, Waterfield CJ, Farrant RD, Nicholson JK. (2002). NMR and pattern recognition studies on liver extracts and intact livers from rats treated with alpha-naphthylisothiocyanate. *Biochem Pharmacol* 64:67–77.
- Waters NJ, Waterfield CJ, Farrant RD, Holmes E, Nicholson JK. (2005). Metabonomic deconvolution of embedded toxicity: application to thioacetamide hepato- and nephrotoxicity. *Chem Res Toxicol* 18:639–654.
- Wei L, Liao P, Wu H, Li X, Pei F, Li W, Wu Y. (2008). Toxicological effects of cinnabar in rats by NMR-based metabolic profiling of urine and serum. *Toxicol Appl Pharmacol* 227:417–429.
- Wei L, Liao P, Wu H, Li X, Pei F, Li W, Wu Y. (2009). Metabolic profiling studies on the toxicological effects of realgar in rats by (1)H NMR spectroscopy. *Toxicol Appl Pharmacol* 234:314–325.
- Wu H, Zhang X, Liao P, Li Z, Li W, Li X, Wu Y, Pei F. (2005). NMR spectroscopic-based metabonomic investigation on the acute biochemical effects induced by Ce(NO<sub>3</sub>)<sub>3</sub> in rats. *J Inorg Biochem* 99:2151–2160.